

Band point algorithms for measuring diffraction pattern parameters in laser ektacytometry of red blood cells

S.Yu. Nikitin, V.D. Ustinov, S.D. Shishkin

Abstract. We consider the issues of measuring the deformability of red blood cells by the method of laser diffractometry in shear flow (ektacytometry). The measurement procedure is optimised taking into account the finite resolution of the video recording system of the laser ektacytometer. An algorithm is proposed that allows one to determine with high accuracy the diffraction pattern parameters necessary for measuring the characteristics of the erythrocyte deformability distribution.

Keywords: deformability of red blood cells, laser diffractometry, data processing algorithms.

1. Introduction

In some diseases, red blood cells with increased rigidity are present in human blood. Such cells do not pass well through the capillaries and impede the delivery of oxygen to the organs and tissues of the body. As an example, we can mention sickle cell anaemia [1], falciparum malaria [2], and hereditary spherocytosis [3]. Reduced deformability of erythrocytes can complicate diabetes mellitus, coronary heart disease, cerebrovascular accident and many other diseases [4]. In this regard, an important task is to measure the deformability of red blood cells [5, 6], as well as to analyse the factors affecting this characteristic of blood cells [7–9]. Fundamental aspects of red blood cell deformability can be studied using techniques that work with individual blood cells, such as aspiration of an erythrocyte into a micropipette, atomic force microscopy, and laser tweezers [10]. Medical applications require techniques to rapidly process large cell ensembles. One of them is laser diffractometry of red blood cells in shear flow (ektacytometry) [11–13].

The idea behind this method is to measure the deformation of blood cells in a given shear stress field. A highly diluted suspension of red blood cells is poured into a gap between the walls of two transparent coaxial cups, one of which is stationary and the other can rotate at a given

angular velocity (a so-called Couette cell). The rotation of the movable cup creates shear stresses in the suspension, which deform red blood cells, pulling them along the flow. The suspension is illuminated with a laser beam and the resulting light scattering pattern – a diffraction pattern – is observed.

In practice, laser ektacytometry of red blood cells is used to diagnose and treat sickle cell anaemia, malaria and other diseases caused by impaired deformability of blood cells. In this case, the task is to measure not only the average deformability, but also the characteristics of the red blood cell deformability distribution, in particular, to determine the fraction of weakly deformable erythrocytes in the blood sample under study [14]. To solve this task, various methods have been considered [15–18]. We have proposed algorithms for processing laser ektacytometry data, which make it possible to measure the characteristics of red blood cell deformability distribution, such as its average value, width and distribution asymmetry [19–22]. One of the algorithms, i.e. the line curvature algorithm, involves measuring the curvature of the iso-intensity line of the diffraction pattern. In this paper, we discuss the optimisation of this procedure taking into account the finite resolution of the video recording system of a laser ektacytometer. To solve this problem, we introduce the concept of a band point of the iso-intensity line, defining it as one of the points on a circle of the line curvature under conditions when the line itself is not precisely determined, but is given as a band of finite width.

2. Diffraction pattern characteristics

Following Refs [19–22], we simulate red blood cells in the shear flow of a laser ektacytometer by elliptical disks with semi-axes a and b . Taking into account the nonuniformity of the red blood cell ensemble, we consider the parameters a and b as random variables and describe them by the formulae $a = a_0(1 + \varepsilon)$ and $b = b_0(1 - \varepsilon)$, where a_0 and b_0 are the average sizes of the semi-axes, and ε is a random parameter, the average value of which is assumed to be zero, i.e., $\langle \varepsilon \rangle = 0$. The measured parameters have the form

$$s = \frac{a_0}{b_0}, \quad \mu = \langle \varepsilon^2 \rangle, \quad \nu = \langle \varepsilon^3 \rangle, \quad (1)$$

which characterise, respectively, the average deformability of red blood cells, the width, and the asymmetry of their deformability distribution.

We represent the light intensity distribution in the diffraction pattern as [22]

S.Yu. Nikitin, S.D. Shishkin Faculty of Physics, Lomonosov Moscow State University, Vorob'evy Gory, 119991 Moscow, Russia; e-mail: sergeynikitin007@yandex.ru;

V.D. Ustinov Faculty of Computational Mathematics and Cybernetics, Lomonosov Moscow State University, Vorob'evy Gory, 119991 Moscow, Russia

Received 10 May 2020; revision received 11 February 2021
Kvantovaya Elektronika 51 (4) 353–358 (2021)
Translated by I.A. Ulitkin

$$\tilde{I}(x, y) = \frac{\langle (ab)^2 G(\xi) \rangle}{\langle (ab)^2 \rangle}$$

or

$$\tilde{I} = \frac{\langle (1 - \varepsilon^2)^2 G(\xi) \rangle}{\langle (1 - \varepsilon^2)^2 \rangle}. \quad (2)$$

Here, angle brackets mean averaging over the ensemble of red blood cells; $\tilde{I} = I/I_0$ is the normalised intensity; I is the light intensity at a given point in the diffraction pattern; I_0 is the intensity of the central diffraction maximum;

$$\xi = \xi(x, y) = \frac{k}{z} \sqrt{a^2 x^2 + b^2 y^2}; \quad (3)$$

x and y are the coordinates of the point of the diffraction pattern; $k = 2\pi/\lambda$ is the wave number; λ is the laser wavelength; z is the distance from the measuring volume to the observation screen;

$$G(\xi) = \left[\frac{2J_1(\xi)}{\xi} \right]^2 \quad (4)$$

is the Airy function; and $J_1(\xi)$ is the first order Bessel function. Formulae (2)–(4) were obtained in the approximation of single scattering and anomalous diffraction; they describe the light intensity distribution in the far diffraction zone in the region of small scattering angles and in that part of the space that lies outside the forward laser beam. A detailed derivation of formulae (2)–(4) is presented in our papers [23–27].

The iso-intensity line of the diffraction pattern is the line on the observation screen, on which the scattered light intensity has a constant value:

$$\tilde{I} = \text{const}. \quad (5)$$

Equations (2)–(5) implicitly define the function $y = y(x)$ or $x = x(y)$, which describes the shape of the iso-intensity line. This line is symmetrical about the Cartesian coordinate axes.

Let us assume that the iso-intensity line shape can be measured using a laser ektacytometer. However, the measurement results will not be very accurate due to the finite resolution of the diffraction pattern. In practice, the iso-intensity line is a set of points in the diffraction pattern, the light intensity in which lies in a small interval near a given

value: $\tilde{I}_0 \leq \tilde{I}(x, y) \leq \tilde{I}_0 + \Delta\tilde{I}$. Thus, the iso-intensity is actually a band of small but finite width (Fig. 1). The limiting width of this band is determined by the resolution of the video recording system of the laser ektacytometer.

The points of intersection of the iso-intensity line with the Cartesian coordinate axes are called polar points; there are only four such points. However, due to the symmetry of the iso-intensity line, it is sufficient to consider two of them, i.e. the upper and right polar points. The upper polar point has coordinates $x = 0$ and $y = y(x = 0) = y_p$, and the right one, $y = 0$, $x = x(y = 0) = x_p$.

To measure the characteristics of the red blood cell deformability distribution, we propose an algorithm based on measuring the curvature of the iso-intensity line at its polar points [22]. The input parameters for this algorithm are dimensionless quantities determined by the formulae

$$C_1 = \sqrt{x(0) \left| \frac{d^2 x}{dy^2} (y = 0) \right|}, \quad C_2 = \sqrt{y(0) \left| \frac{d^2 y}{dx^2} (x = 0) \right|}.$$

The measurement of C_1 and C_2 is complicated by the fact that in practice the iso-intensity line is a band of finite width. This circumstance reduces the accuracy with which the parameters of the iso-intensity line curvature, as well the desired characteristics of the red blood cell deformability, can be determined.

3. Band point algorithm

In [28], we proposed a method for measuring the iso-intensity line curvature based on the concept of a band point. One of the points of the circle of curvature of the curve under the conditions when this curve is specified in the form of a band of finite width is what we call a band point. Let us consider the band point algorithm using the example of the upper polar point of the iso-intensity line. The iso-intensity line curvature parameter at its upper polar point is defined as

$$C_2 = \frac{y_p}{x_2} \sqrt{2 \left| \frac{y_2}{y_p} - 1 \right|}. \quad (6)$$

Here x_2 and $y_2 = y(x_2)$ are the coordinates of the band point, and

$$x_2 = 2x_p^4 \sqrt{\frac{\Delta y}{y_p}}, \quad (7)$$

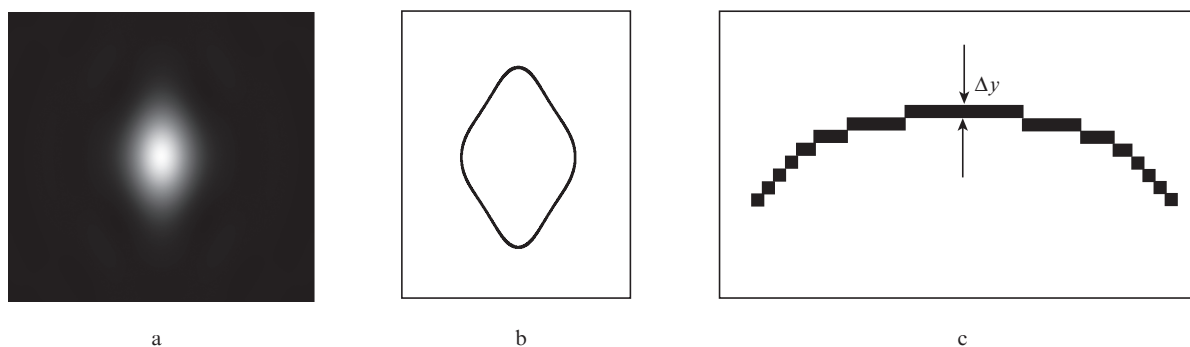


Figure 1. (a) Diffraction pattern, (b) iso-intensity line and (c) fine structure of this line near its upper polar point; Δy is the vertical size of one pixel of the diffraction pattern.

where Δy is the iso-intensity line width. The error in measuring the parameter C_2 according to formula (6) does not exceed

$$\delta C_2 = \sqrt{\frac{\Delta y}{y_p}}. \tag{8}$$

It is seen that this error increases with increasing line width Δy . Its minimum possible width Δy_{\min} is determined by the resolution of the video recording system of the laser ektacytometer, i.e. $\Delta y_{\min} = y_p/N_y$, where N_y is the number of pixels in the diffraction pattern in the area from the pattern centre to the upper polar point of the iso-intensity line. The minimum error in measuring the iso-intensity line curvature is $\delta C_2 = 1/\sqrt{N_y}$. For example, if $N_y = 10^4$, then $\delta C_2 = 1\%$. The polar and band points of the iso-intensity line are shown in Fig. 2.

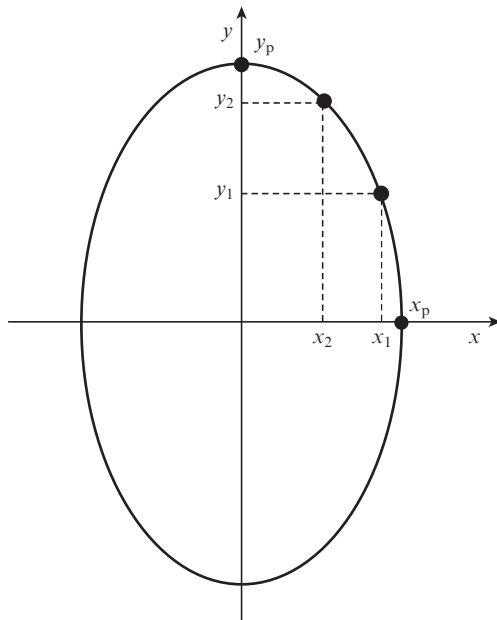


Figure 2. Polar and band points on the iso-intensity line.

The estimates given in [28] should be regarded as approximate, because they are obtained on the basis of an approximate formula for the iso-intensity line curvature. More accurate data can be obtained based on numerical calculations. The purpose of this work is to verify and refine the band point algorithm proposed in [28]. In particular, formula (7) for the coordinate of the band point needs to be refined.

Following [22], we introduce the parameter $c_0 = \sqrt{a_0 b_0}$ and the normalised coordinates

$$U = \sqrt{s} \frac{k}{z} c_0 x, \quad V = \frac{1}{\sqrt{s}} \frac{k}{z} c_0 y. \tag{9}$$

Here the parameter s is determined by formula (1). In these coordinates, taking into account (3), ξ takes the form:

$$\xi = \sqrt{(1 + \varepsilon)^2 U^2 + (1 - \varepsilon)^2 V^2}. \tag{10}$$

Formulae (2), (5), and (10) implicitly define the function $V = V(U)$ or $U = U(V)$, which describes the form of the iso-intensity line. The iso-intensity line curvature parameter near its upper polar point is written in the form

$$C_2 = s \sqrt{|V(0) V''(0)|}.$$

Using the band point algorithm, this parameter can be calculated by the formula

$$C_2 = s \frac{V_p}{U_2} \sqrt{2 \left| \frac{V_2}{V_p} - 1 \right|}. \tag{11}$$

To perform numerical calculations, it is necessary to select a specific model of an ensemble of red blood cells in the shear flow of a laser ektacytometer. One of the simplest models is a bimodal ensemble, which contains only two types of cells (rigid and soft erythrocytes). Let the cells of the first type be characterised by the aspect ratio $s_1 = a_1/b_1$, and the second type, by the aspect ratio $s_2 = a_2/b_2$. The fraction of cells of the first type in the ensemble will be denoted as p . Without loss of generality, we will assume that $s_1 < s_2$. In this model, the erythrocyte shape parameters ε_1 and ε_2 , according to [19], take the form

$$\varepsilon_1 = \frac{s_1 - s}{s_1 + s}, \quad \varepsilon_2 = \frac{s_2 - s}{s_2 + s}. \tag{12}$$

Here

$$s = M + \sqrt{M^2 + s_1 s_2}, \quad M = (s_1 - s_2) \left(p - \frac{1}{2} \right). \tag{13}$$

The light intensity distribution in the diffraction pattern is described by the expression

$$\tilde{I} = \frac{p(1 - \varepsilon_1^2)^2 G(\xi_1) + (1 - p)(1 - \varepsilon_2^2)^2 G(\xi_2)}{p(1 - \varepsilon_1^2)^2 + (1 - p)(1 - \varepsilon_2^2)^2}, \tag{14}$$

where

$$\xi_1 = \sqrt{(1 + \varepsilon_1)^2 U^2 + (1 - \varepsilon_1)^2 V^2}, \tag{15}$$

$$\xi_2 = \sqrt{(1 + \varepsilon_2)^2 U^2 + (1 - \varepsilon_2)^2 V^2}.$$

When condition (5) is satisfied, we find the iso-intensity line using formulae (14) and (15).

The coordinate of the upper polar point of this line, $V_p = V(U = 0)$, is determined by the equation

$$\tilde{I} = p(1 - \varepsilon_1^2)^2 G[(1 - \varepsilon_1) V_p] + (1 - p)(1 - \varepsilon_2^2)^2 G[(1 - \varepsilon_2) V_p] \times [p(1 - \varepsilon_1^2)^2 + (1 - p)(1 - \varepsilon_2^2)^2]^{-1}, \tag{16}$$

and the coordinate of the right polar point, $U_p = U(V = 0)$, is determined by the equation

$$\tilde{I} = p(1 - \varepsilon_1^2)^2 G[(1 + \varepsilon_1) U_p] + (1 - p)(1 - \varepsilon_2^2)^2 G[(1 + \varepsilon_2) U_p] \times [p(1 - \varepsilon_1^2)^2 + (1 - p)(1 - \varepsilon_2^2)^2]^{-1}. \tag{17}$$

The equation for the coordinate of the upper band point

$$V_2 = V(U_2) \tag{18}$$

has the form

$$\tilde{I} = \frac{p(1 - \varepsilon_1^2)^2 G(\xi_1) + (1 - p)(1 - \varepsilon_2^2)^2 G(\xi_2)}{p(1 - \varepsilon_1^2)^2 + (1 - p)(1 - \varepsilon_2^2)^2}, \quad (19)$$

where

$$\begin{aligned} \xi_1 &= \sqrt{(1 + \varepsilon_1)^2 U_2^2 + (1 - \varepsilon_1)^2 V_2^2}, \\ \xi_2 &= \sqrt{(1 + \varepsilon_2)^2 U_2^2 + (1 - \varepsilon_2)^2 V_2^2}. \end{aligned} \quad (20)$$

The transcendental equation (19) for the coordinate of the band point V_2 can be solved numerically with any accuracy by choosing a sufficiently small step ΔV_2 of changing the coordinate V_2 . Let us restrict ΔV_2 by the condition

$$\Delta V_2 = \frac{V_p}{N_y}. \quad (21)$$

In doing so, we admit inaccuracy in determining the coordinates of the band point in order to take into account the finite width of the iso-intensity line. The number N_y in (21) characterises the resolution of the diffraction pattern and is a calculation parameter. Another parameter of the calculation is the coordinate of the band point, U_2 , in formulae (11) and (20).

We compare the result of calculating C_2 with the exact value of this parameter, which we find by the formulae [22]

$$C_{2\text{ex}} = s \sqrt{\frac{g_{1V} G'[(1 - \varepsilon_1) V_p] + g_{2V} G'[(1 - \varepsilon_2) V_p]}{h_{1V} G'[(1 - \varepsilon_1) V_p] + h_{2V} G'[(1 - \varepsilon_2) V_p]}}, \quad (22)$$

$$\begin{aligned} g_{1V} &= (1 - \varepsilon_1)(1 + \varepsilon_1)^4 p, \\ g_{2V} &= (1 - \varepsilon_2)(1 + \varepsilon_2)^4 (1 - p), \\ h_{1V} &= (1 - \varepsilon_1)^3 (1 + \varepsilon_1)^2 p, \\ h_{2V} &= (1 - \varepsilon_2)^3 (1 + \varepsilon_2)^2 (1 - p). \end{aligned} \quad (23)$$

The function $G'(\xi)$ is defined as

$$G'(\xi) = \frac{dG}{d\xi} = \frac{8}{\xi^3} [\xi J_0(\xi) - 2J_1(\xi)] J_1(\xi). \quad (24)$$

The error in measuring the iso-intensity line curvature using the band point algorithm is found by the formula

$$\delta C_2 = \frac{|C_2 - C_{2\text{ex}}|}{C_{2\text{ex}}} 100\%. \quad (25)$$

4. Verification of the algorithm in a numerical experiment

The procedure for verifying the band point algorithm is as follows. By setting the erythrocyte ensemble parameters s_1 , s_2 , and p , we find the ensemble characteristics s , ε_1 , and ε_2 by formulae (12) and (13). Then, using formulae (14) and (15), we find the distribution of light intensity in the diffraction

pattern arising from the scattering of a laser beam by an ensemble of red blood cells. When condition (5) is met, these formulae describe the iso-intensity line, which is characterised by the normalised light intensity \tilde{I} . By solving numerically equations (16) and (17), we determine the coordinates of the polar points of this line, V_p and U_p . Then we find the exact value of the iso-intensity line curvature parameter at its upper polar point, $C_{2\text{ex}}$, using formulae (22)–(24).

Thus, the exact value of the parameter of the iso-intensity line curvature, $C_{2\text{ex}}$, has been determined. Now we find the value of the parameter C_2 using the band point algorithm, taking into account the finite width of the iso-intensity line. The width of the line, ΔV_2 , near its upper polar point is determined by formula (21). We select the coordinate of the upper band point, U_2 , and find the second coordinate of this point, V_2 , numerically with formulae (19) and (20); in this case, we change the value of V_2 with a step equal to ΔV_2 . In this case, the coordinate V_2 is determined not exactly, but with an error equal to the iso-intensity line width. We substitute the obtained coordinate values into formula (11) and find the value of the parameter of the iso-intensity line curvature, C_2 , under the conditions when this line is given in the form of a band of finite width. The parameters of this calculation are the quantity N_y in formula (21), which characterises the resolution of the diffraction pattern, as well as the normalised coordinate of the upper band point, $U_2/U_p = x_2/x_p$. After that, we estimate the error of the band point algorithm using formula (25).

The calculation results are presented in Fig. 3, which demonstrates the measurement error of the curvature parameter of the iso-intensity line as a function of its width and the choice of the band point coordinate. The abscissa shows the ratio of the band point coordinate x_2 to the coordinate x_p of the iso-intensity line polar point, and the ordinate shows the error in measuring the line curvature parameter at the upper polar point δC_2 , obtained using the band point algorithm under conditions when the iso-intensity line is a band of finite width. The width of this band is determined by formula (21). The straight horizontal line indicates an error level of 1%. The found dependence can be compared with the approximate dependence given in [28] and expressed by formula

$$\delta C_2 = \frac{1}{2} \left[\frac{1}{N_y} \left(\frac{2x_p}{x_2} \right)^2 + \left(\frac{x_2}{2x_p} \right)^2 \right]$$

(shown in the figure by a dashed line). The data presented in Fig. 3 refer to the upper band point of the iso-intensity. Similar results were obtained for the right band point.

The calculation results are presented in more detail in Table 1; use is made of the following notations: s_1 is the aspect ratio for the first component of the erythrocyte ensemble, s_2 is the aspect ratio for the second component of the erythrocyte ensemble, p is the fraction of particles of the first type in the ensemble, N_x is the resolution of the video recording system of the laser ektacytometer along the horizontal axis, y_1 is the vertical coordinate of the right band point of the iso-intensity line, x_2 is the horizontal coordinate of the upper band point, x_p is the coordinate of the right polar point of the iso-intensity line, y_p is the coordinate of the upper polar point (these points are shown in Fig. 2), δC_1 is the measurement error of the parameter of the iso-intensity line curvature at the right polar point, and δC_2 is measurement error of the parameter of the iso-intensity line curvature at the upper polar point. In all

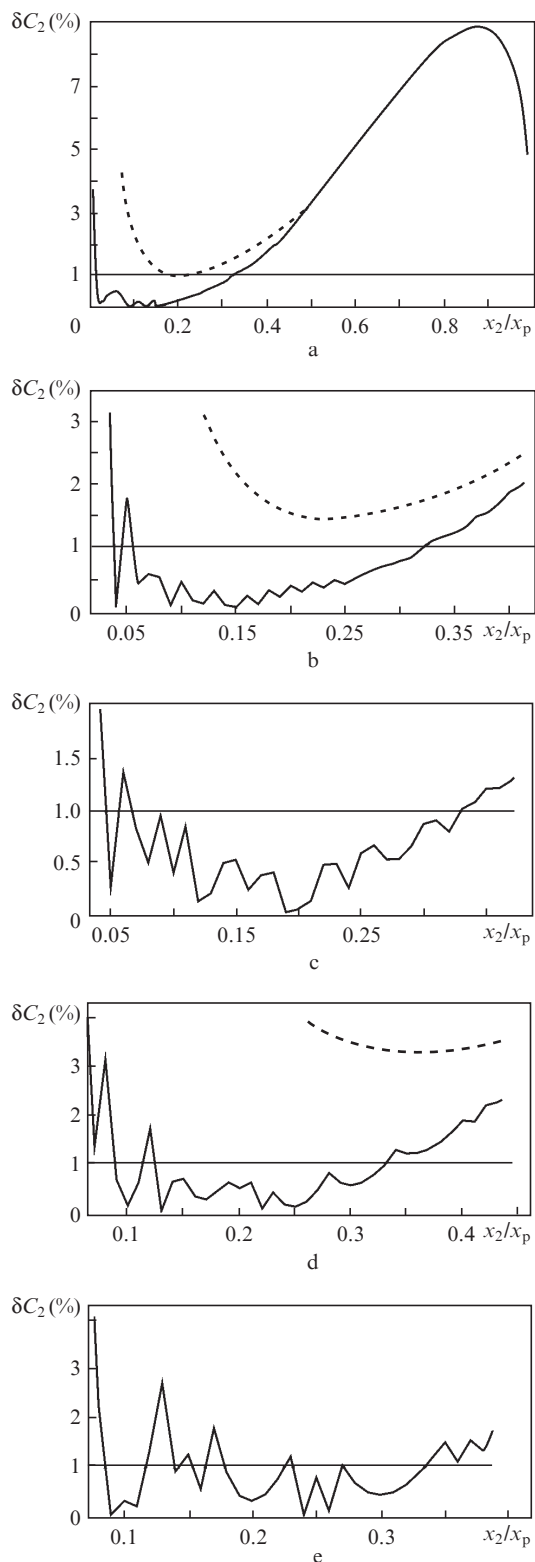


Figure 3. Error in measuring the curvature of the iso-intensity line as a function of the coordinate of the band point. Calculation parameters are as follows: (a) $s_1 = 1, s_2 = 2, p = 0.5, \bar{I} = 0.05, N_x = 10^4$; (b) $s_1 = 1, s_2 = 2, p = 0.5, \bar{I} = 0.05, N_x = 5000$; (c) $s_1 = 1, s_2 = 2, p = 0.5, \bar{I} = 0.05, N_x = 2000$; (d) $s_1 = 1, s_2 = 2, p = 0.5, \bar{I} = 0.05, N_x = 1000$; and (e) $s_1 = 1, s_2 = 2, p = 0.5, \bar{I} = 0.05, N_x = 500$.

cases, we assumed the same resolution of the video recording system along the horizontal and vertical axes, i.e. $N_x = N_y$; the level of light intensity at the iso-intensity line is $\bar{I} = 0.05$.

Table 1. Numerical results.

Calculation parameter				Coordinates of band points	
s_1	s_2	p	N_x	y_1/y_p ($\delta C_1 < 1\%$)	x_2/x_p ($\delta C_2 < 1\%$)
1.0	2.0	0.5	10^4	0.02–0.33	0.02–0.33
1.0	2.0	0.5	5000	0.06–0.33	0.06–0.33
1.0	2.0	0.5	2000	0.07–0.33	0.07–0.33
1.0	2.0	0.5	1000	0.13–0.33	0.13–0.33
1.0	2.2	0.5	2000	0.08–0.34	0.08–0.34
1.0	2.5	0.5	2000	0.09–0.17	0.09–0.17
1.5	3.0	0.5	2000	0.07–0.33	0.07–0.33
1.0	2.0	0.4	2000	0.09–0.18	0.09–0.61
1.0	2.0	0.3	5000	0.07–0.15	0.07–0.31
1.0	2.0	0.2	5000	0.07–0.15	0.06–0.29
1.0	2.0	0.1	5000	0.07–0.27	0.07–0.27
1.0	2.0	0.05	5000	0.07–0.56	0.07–0.26
1.0	2.0	0	5000	0.06–0.27	0.06–0.26

5. Discussion and results

Numerical experiments carried out on the model of a bimodal ensemble of red blood cells show that, under typical experimental conditions, the band point algorithm makes it possible to measure the parameters of the iso-intensity line curvature with an error not exceeding 1% (see Fig. 3 and Table 1). In this case, as a rule, it is sufficient to have the resolution of the laser ektacytometer, characterised by the numbers $N_x = N_y = 2000$. Only in some cases, to achieve such an accuracy of measurements, a resolution at a level of $N_x = N_y = 5000$ is required. Thus, provided the diffraction pattern is of good quality, the band point algorithm provides an accuracy sufficient for practical applications.

Analysis of the data obtained allows us to conclude that the optimal values of the coordinates of the band points are determined by the formulae

$$y_1 = y_p \sqrt[4]{\frac{\Delta x}{x_p}}, \quad x_2 = y_p \sqrt[4]{\frac{\Delta y}{y_p}}.$$

Here x_p and y_p are the coordinates of the polar points, and Δx and Δy are the widths of the iso-intensity line near the polar points. The minimum values of Δx and Δy are determined as

$$\Delta x = \frac{x_p}{N_x}, \quad \Delta y = \frac{y_p}{N_y},$$

where N_x and N_y are the number of pixels in the diffraction pattern along the horizontal and vertical axes, respectively. In this case,

$$y_1 = \frac{y_p}{\sqrt[4]{N_x}}, \quad x_2 = \frac{x_p}{\sqrt[4]{N_y}}. \tag{26}$$

For example, if $N_x = N_y = 2000$, then $y_1 = 0.15y_p$ and $x_2 = 0.15x_p$.

6. Conclusions

The problem of measuring the curvature of iso-intensity lines of diffraction patterns in laser ektacytometry of red blood

cells is considered. These parameters are the input data for the algorithm [22], which makes it possible to measure the characteristics of erythrocyte deformability based on laser ektacytometry data. The finite resolution of the diffraction pattern leads to the fact that, in practice, the iso-intensity line is a band of finite width. To measure the curvature of such a line, we have proposed an algorithm based on the concept of a band point. We call a band point one of the points of the circle of curvature of a line under conditions when this line itself is not precisely defined, but is specified as a band of finite width. Our proposed algorithm for measuring the iso-intensity line curvature of the diffraction pattern is expressed by the formulae

$$C_1 = \frac{x_p}{y_1} \sqrt{2 \left| \frac{x_1}{x_p} - 1 \right|}, \quad C_2 = \frac{y_p}{x_2} \sqrt{2 \left| \frac{y_2}{y_p} - 1 \right|},$$

where C_1 and C_2 are the parameters of the curvature of the line at its polar points; x_p and y_p are coordinates of polar points; x_1 , y_1 and x_2 , y_2 are the coordinates of the band points of the iso-intensity line (see Fig. 2). Approximate analytical expressions for the coordinates of band points were obtained in our work [28]. In this work, based on the data of a numerical experiment, the estimates are refined and it is concluded that the optimal choice of the coordinates of the band points is determined by formulae (26), where the numbers N_x and N_y characterise the resolution of the video recording system of a laser ektacytometer along two coordinate axes.

Note that the measurement of the curvature of the iso-intensity line using the band point algorithm requires a minimum amount of information: the coordinates of four polar points and eight band points of the iso-intensity line. This simplifies the procedure for measuring the characteristics of erythrocyte deformability based on laser ektacytometry, proposed in [22].

Acknowledgements. This work was supported by the Russian Science Foundation (Grant No. 18-71-00158).

References

- Rabai M., Detterich J.A., Wenby R.B., Hernandez T.M., Toth K., Meiselman H.J., Wood J.C. *Biorheology*, **51** (2–3), 159 (2014).
- Dondorp A.M., Angus B.J., Hardeman M.R., Chotivanich K.T., Silamut K., Ruangveerayuth R., Kager P.A., White N.J., Vreeken J. *Am. J. Trop. Med. Hyg.*, **57** (5), 507 (1997).
- Da Costa L., Galimand J., Fenneteau O., Mohandas N. *Blood Rev.*, **27** (4), 167 (2013).
- Toth K., Kesmarky G., Alexy T., in *Handbook of Hemorheology and Hemodynamics*. Ed. by O.K. Baskurt, M.R. Hardeman, M.W. Rampling, H.J. Meiselman (Amsterdam: IOS Press, 2007) pp 392–432.
- Zinchuk V.V. *Usp. Fiziol. Nauk.*, **32** (3), 64 (2001).
- Huisjes R., Bogdanova A., van Solinge W.W., Schiffelers R.M., Kaestner L., van Wijk R. *Front. Physiol.*, **9**, 656 (2018).
- Muravyov A.V., Mikhailov P.V., Tikhomirova I.A. *Region. Krovoobrashch. Mikrotsirk.*, **16** (2), 90 (2017).
- Muravyov A.V., Tikhomirova I.A. *Clin. Hemorheol. Microcirc.*, **53**, 45 (2013).
- Semenov A.N., Shirshin E.A., Muravyov A.V., Priezzhev A.V. *Front. Physiol.*, **10**, 923 (2019).
- Kim Y., Kim K., Park Y., in *Blood Cell – An Overview of Studies in Hematology*. Ed. by T.E. Moschandreu (InTech, 2012) pp 167–195.
- Bessis M., Mohandas N. *Blood Cells*, **1**, 307 (1975).
- Baskurt O.K., Hardeman M.R., Uyuklu M., Ulker P., Cengiz M., Nemeth N., Shin S., Alexy T., Meiselman H. *J. Biorheology*, **46**, 251 (2009).
- Firsov N.N., Dzhanashia P.Kh. *Vvedenie v eksperimental'nyu i klinicheskuyu gemoreologiyu* (Introduction to Experimental and Clinical Hemorheology) (Moscow: RGMU, 2008).
- Renoux C., Parrow N., Faes C., Joly P., Hardeman M., Tisdale J., Levine M., Garnier N., Bertrand Y., Kebaili K., Cuzzubbo D., Cannas G., Martin C., Connes P. *Clin. Hemorheol. Microcirc.*, **62**, 173 (2016).
- Plasek J., Marik T. *Appl. Opt.*, **21** (23), 4335 (1982).
- Streekstra G.J., Dobbe J.G.G., Hoekstra A.G. *Opt. Express*, **18** (13), 14173 (2010).
- Rabai M., Meiselman H.J., Wenby R.B., Detterich J.A., Feinberg J. *J. Biorheology*, **49**, 317 (2012).
- Rab M.A.E., Oirschot B.A., Bos J., Merck T.H., Wesel A.C.W., Abdulmalik O., Safo M.K., Versluijs B.A., Houwing M.E., Cnossen M.H., Riedl J., Schutgens R.E.G., Pasterkamp G., Bartels M., Beers E.J., Wijk R. *Am. J. Hematol.*, **94**, 575 (2019).
- Nikitin S.Yu., Priezzhev A.V., Lugovtsov A.E., Ustinov V.D., Razgulina A.V. *J. Quant. Spectrosc. Radiat. Transfer*, **146**, 365 (2014).
- Nikitin S.Yu., Ustinov V.D., Yurchuk Yu.S., Lugovtsov A.E., Lin M.D., Priezzhev A.V. *J. Quantum. Spectrosc. Radiat. Transfer*, **178**, 315 (2016).
- Nikitin S.Yu., Ustinov V.D., Tsybrov E.G., Priezzhev A.V. *Izv. Saratov Univ., Novaya Seriya. Ser. Fiz.*, **17** (3), 150 (2017); DOI: 10.18500/1817-3020-2017-17-3-150-157.
- Nikitin S.Yu., Ustinov V.D., Shishkin S.D., Lebedeva M.S. *Quantum Electron.*, **50** (9), 888 (2020) [*Kvantovaya Elektron.*, **50** (9), 888 (2020)].
- Nikitin S.Yu., Priezzhev A.V., Lugovtsov A.E., in *Advanced Optical Flow Cytometry: Methods and Disease Diagnoses*. Ed. by V.V. Tuchin (Wiley, 2011) pp 133–154.
- Nikitin S.Yu., Lugovtsov A.E., Priezzhev A.V. *Quantum Electron.*, **40** (12), 1074 (2010) [*Kvantovaya Elektron.*, **40** (12), 1074 (2010)].
- Nikitin S.Yu., Lugovtsov A.E., Priezzhev A.V., Ustinov V.D. *Quantum Electron.*, **41** (9), 843 (2011) [*Kvantovaya Elektron.*, **41** (9), 843 (2011)].
- Nikitin S.Yu., Priezzhev A.V., Lugovtsov A.E. *J. Quant. Spectrosc. Radiat. Transfer*, **121**, 1 (2013).
- Nikitin S.Yu. *Doct. Dis. (Saratov, SSU)*, 2016.
- Nikitin S.Yu., Ustinov V.D., Shishkin S.D. *J. Quant. Spectrosc. Radiat. Transfer*, **235**, 272 (2019).